

Structural Parameters Analysis of Mg Doped ZnO Nano Particles for Various Mg Concentrations

Shanmugan S^{1*}, Mohamed Mustaqim A.B² and Mutharasu D¹

¹Nano Optoelectronics and Research Laboratory,

²X-Ray Crystallography Lab, School of Physics,

Universiti Sains Malaysia (USM), 11800, Minden, Penang, Malaysia

Abstract – Mg doped ZnO nano particles were synthesized by chemical precipitation method and post processing was performed at two different annealing temperatures. The structural characterization was performed for all Mg doped ZnO samples using XRD and their results were compared with the results of undoped ZnO nano particles. As grown samples were the mixture of randomly orientated ZnO nano crystals along with Zn(OH)₂ compounds and confirmed by XRD spectra. Annealing process was aided to decompose Zn(OH)₂ compounds and observed pure ZnO compounds with preferred (100), (002) and (101) orientations. The peak intensity of preferred orientations was varied with respect to Mg concentrations and low for the samples of 6% M Mg (6MZO) annealed at 500°C. Highly intensive peak was noticed for 700°C annealed samples. Peak shifting towards low and high 2θ values was noticed for 6MZO samples annealed at 500°C and 700°C respectively. Mg doping was influenced the crystallite size of ZnO nanoparticles and low value was observed with 6MZO sample. The lattice parameters of undoped and Mg doped ZnO nano particles were slightly changes with respect to the Mg concentrations and higher value was noticed with ≥8 M% of Mg in ZnO. The dislocation density was also dependent on Mg concentrations as well as annealing temperatures and low values were noticed with low Mg concentrations for (002) oriented phase at annealed conditions. As grown samples were influenced by the mixture of tensile and compressive stress and high & low values in tensile stress were noticed with (002) orientate of 6MZO samples (9.18×10^{-2}) and (100) orientation of 2MZO samples (8.76×10^{-4}) respectively when annealed at 700°C.

Keywords — ZnO, nano particles, XRD, Mg doping, structural analysis

I. INTRODUCTION

Nanoscale materials experience dramatically increased surface area compared to their bulk counterpart of similar mass. One benefit of greater surface area can dramatically improve the reactivity of surface dependent chemical processes especially catalysis. Nanoengineered catalysts have benefited the oil and chemical industries. Reactions in energy technology products such as batteries, fuel cells, etc can potentially enhanced by incorporating

nanomaterials. In fact, physical and chemical properties of nanoscale materials are size dependent and this offers the possibility for researchers to fine-tune a material property of interest to suite their application [1]. ZnO is an important ingredient in many pharmaceutical and cosmetic products such as medicine, dental paste filler, nutritional products and diet supplements. ZnO also applied to UV protection products such as sun cream and UV-blocking textiles. ZnO also been used as catalyst in chemical industry, fire and water resistance additive in paint, cigarette filters, etc. [2].

Nanogenerators based on ZnO also become a new candidate for future green energy harvesting technology [3]. Moreover, manganese doped ZnO is found to be a dilute magnetic semiconductors (DMS) which exhibit room temperature ferromagnetism. Such a novel property of the material has opened up a new possibility for applications in spin transfer electronics which is also known as spintronics [4]. Bulk ZnO have high mechanical and thermal stability, with modulus of hardness and melting point of 4-5 and 1975°C respectively. It also has fairly high thermal conductivity of about 1-1.2 Wcm⁻¹K⁻¹ at room conditions [5,6]. The thermal expansion coefficient (CTE) of ZnO at 300K along *a* and *c* axes are 4.31×10^{-6} K⁻¹ and 2.49×10^{-6} K⁻¹ respectively. Meanwhile, the specific heat capacity at constant pressure of ZnO is $c_p=40.3$ Jmol⁻¹K⁻¹. However, thermal conductivity and specific heats at low temperature may vary significantly depending on the defects present [7]. In addition, metal doping also induce some defects in ZnO lattice during the process time. Consequently, a detailed study on the structural parameters should be addressed to optimize the synthesis parameter of ZnO nano particles for suitable application.

There have been many methods for the synthesis of ZnO nano particles and also for doping. For the synthesis of ZnO nano particles, mostly reported methods are from sol-gel [8], precipitation [9], hydrothermal [10], solvothermal [11], mechanochemical [2], spray pyrolysis [12], etc. Among these methods, precipitation method is a best method and also cost effective. The process can be controlled easily. In this work, Mg was used as dopant to ZnO and their structural parameters such as crystallite size, residual stress, strain, dislocation density, texture coefficient, lattice parameters etc were

analysed and explained the influence of Mg on the same.

II. EXPERIMENTAL TECHNOLOGY

Mg doped ZnO nano particles were synthesized by precipitation method. Zinc Nitrate Hexahydrate $Zn(NO_3)_2 \cdot 6H_2O$ (Sigma Aldrich), Sodium Hydroxide NaOH (Sigma Aldrich) and Magnesium Chloride Hexahydrate $MgCl_2 \cdot 6H_2O$ (QR&C™), were AR grade and used in the synthesis of Mg-doped Zinc Oxide without further purification. For synthesis of pure ZnO, 29.749g of $Zn(NO_3)_2 \cdot 6H_2O$ and 8.00g of NaOH were dissolved separately in 200ml of double distilled water to prepare 0.5M and 1.0 M solutions respectively.

In all the literature, NaOH is added into zinc solution. Instead, the zinc solution is added into the NaOH solution in this study. This is to ensure the dissolution of zinc hydroxide precipitate into zinc complex ion which can serves as self-assembly units as well as providing an alkaline environment for reaction [13].

TABLE I

SAMPLE NAME AND MG DOPING CONCENTRATIONS

Sample Name	Atomic Percentage (% mol) of $MgCl_2 \cdot 6H_2O$
0MZO	0 (pure ZnO)
2MZO	2
4MZO	4
6MZO	6
8MZO	8
10MZO	10

Consequently, NaOH solution was stirred by mechanical stirrer at 500 rpm and $Zn(NO_3)_2 \cdot 6H_2O$ solution was added dropwise to it to form white precipitates. The titration took about 1.5 hours to complete and the resulting solution was allowed to age for 2 hours. The precipitate was then filtered out, washed for 3-4 times with double distilled water and ethanol successively to remove unwanted solutions. Later, the precursor was dried in oven at 120°C for 4 hours, crushed into powder using ceramic mortar and filtered. The pure ZnO nanopowder was obtained. For Mg doping, $MgCl_2 \cdot 6H_2O$ solution is added along with $Zn(NO_3)_2 \cdot 6H_2O$ and prepared solution. In order to change the atomic concentration of Mg into the ZnO, the weight of $MgCl_2 \cdot 6H_2O$ was varied and mixed with $Zn(NO_3)_2 \cdot 6H_2O$ to achieve the doping concentration as mentioned in table – 1. Later, the as-synthesized and Mg doped samples were annealed at two different temperatures (500°C and 700°C) in a furnace for about 2 hours at air atmosphere with the heating rate of 10°C/min. For sample naming, the sample name in which the front number represents the Mg doping percentage and the number behind represent the annealing temperatures of the sample. For example 2MZO-5 represents 0.2 M Mg doped ZnO annealed at

500°C. Hereafter, the sample name is pronounced based on this nomenclature. The structural properties of the synthesized powder were analysed by using X-Ray Diffractometry (XRD) (Bruker D8 ADVANCE XRD) machine with Cu target ($K\alpha$ wavelength $\lambda=1.5406 \text{ \AA}$) working at 40kV, 40mA.

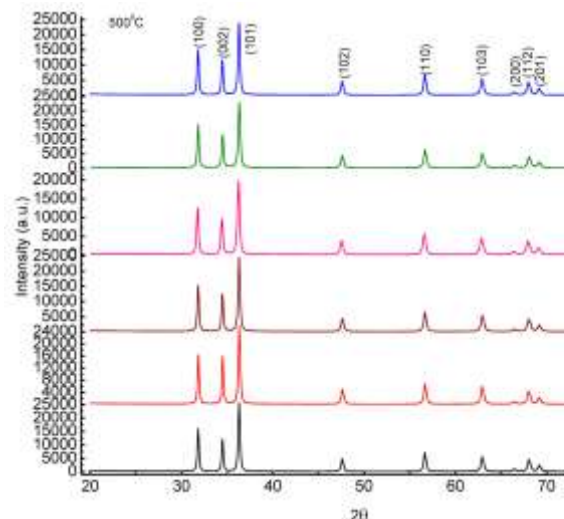


Fig 2. XRD spectra of annealed (500°C) undoped and Mg doped ZnO nano particles for various Mg concentrations

The scanning 2θ range is 20°-80° in steps of 0.02°. From the XRD spectra, the structural parameters such as dislocation density, residual stress, micro strain, crystallite size, lattice parameters, texture coefficient, etc. were calculated and presented for undoped and Mg doped ZnO nano particles.

III. RESULTS AND DISCUSSION

A. XRD spectra analysis

The XRD spectra of as synthesized samples were recorded as shown in fig.1 and indexed by using the XRD software and JCPDS file. It reveals that there are many non-indexed peaks and claimed the presence of $Zn(OH)_2$ phases in the as synthesized samples (JCPDS

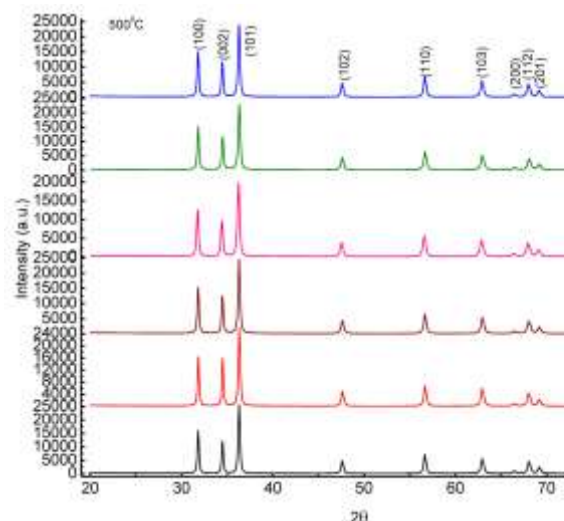


Fig 3. XRD spectra of annealed (700°C) undoped and Mg doped ZnO nano particles for various Mg concentrations

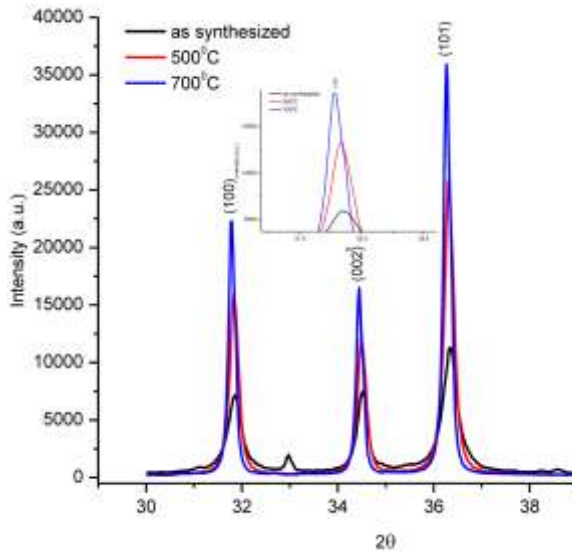


Fig 4. Variation in the intensity of predominated XRD peaks {(100), (002), (101)} of ZnO phase for undoped ZnO nano particles at various annealed temperatures. Inset shows the peak shift for (100) oriented peak

No.890138) before and after doping with Mg. It is also noticed that the $Zn(OH)_2$ peaks are not observed for the samples with moderate Mg concentrations (2MZO & 4MZO). Fig.1 also exhibits the effect of Mg

concentration on the intensity of preferred ZnO peaks such as (100), (002) and (101) orientations. This is due to the fact that ZnO and MgO are belong to different types of lattice (rocksalt type lattice for MgO) [14], which implies that the doping of Mg introduces a certain amount of defects in ZnO host lattice [15]. From the XRD spectra, the growth of crystals towards (101) orientation was suppressed by low and high concentrations of Mg in the ZnO lattice. But noticeable improvement in crystalline quality was noticed with the samples of 4MZO and 6MZO. The same trend was observed with other two preferred orientations {(100), (002)}. From the fig.1, it clearly seen that the other $Zn(OH)_2$ phases are due to the insufficient reaction temperatures during the doping process. It should be avoided to get pure ZnO and Mg doped ZnO and is possible by means of annealing process after the synthesis of undoped and doped ZnO nano particles. Moreover, the annealing process is also suggested to change the crystallite size of the materials usually the bigger size particles are possible. Not only for change in crystallite size, it will also support for the atomic diffusion process and hence the expected doping occurs.

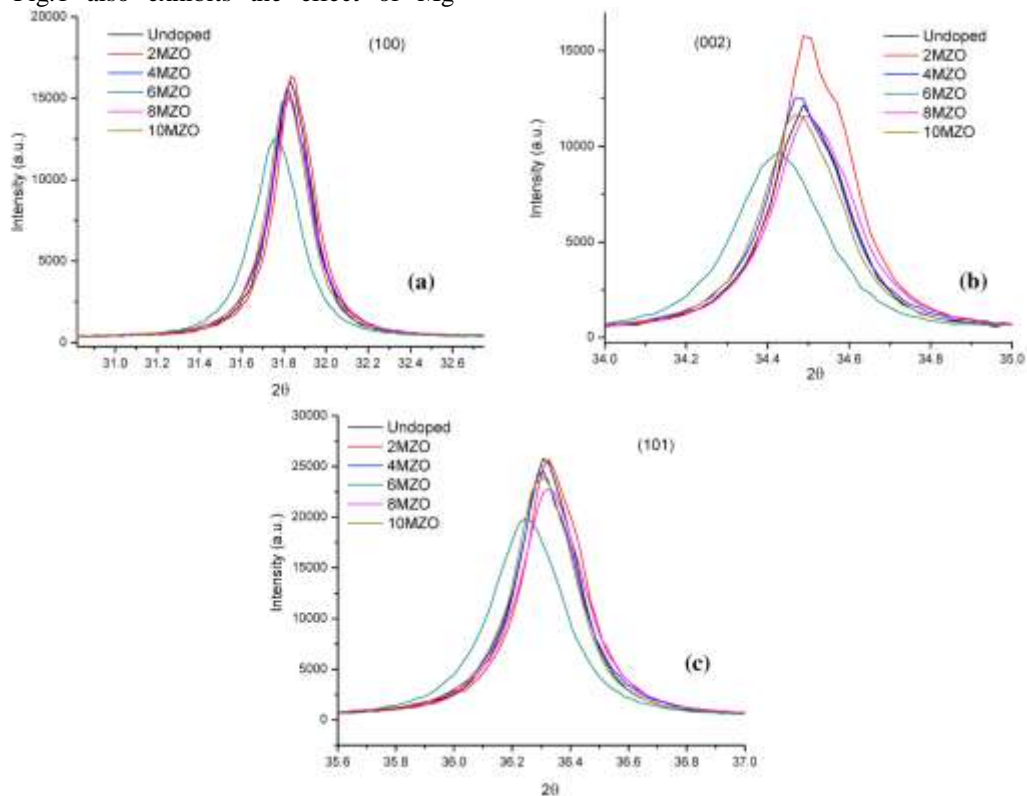


Fig 5. XRD spectra of (100), (002) & (101) oriented peaks of ZnO phases observed from 500°C annealed undoped and Mg doped ZnO nano particles

Consequently, the as synthesized samples were undergone to annealing process at two different temperatures (500 and 700°C) and captured the XRD spectra for all samples as shown in fig.2 and fig.3. It clearly exhibits the pure ZnO crystalline

phases and no more secondary phases such as $Zn(OH)_2$ and MgO are observed after annealing process. It is attributed to the decomposition of amorphous $Zn(OH)_2$ at high annealing temperatures > 450°C [14]. Using the XRD

software, all peaks are indexed and clearly show the variation of intensity of preferred orientations. In order to explain, the effect of annealing on the intensities of preferred orientations for undoped ZnO nano particles are depicted in fig.4 where noticeable increment in intensity could be observed as the annealing temperature increases. However, the variation in the peak intensities shows no strong correlation with the Mg doping (see fig.5a – 5c).

From the fig.5, it is clearly seen that the intensity of 6MZO was low for all preferred orientations and a small change in intensity was noticed with (002) and (101) orientations. For (002) orientations, 2MZO sample shows high intense peak than all samples (see fig.5b). This may be due to the inhomogeneous Mg distribution in the samples. In addition to this, the peak shift as a

result of annealing was also considered in this analysis. For as grown sample (undoped), it is observed from the fig.4 (inset) that (100) oriented peak shift towards lower 2θ as a result of annealing. The same behaviour could also be observed for all other predominated peaks of (002) and (101) orientations. It clearly shows that the peak shifting towards lower diffraction angle with high intensity which implying a good crystalline structure of the ZnO nanoparticles product. In addition to this, the effect of Mg doping on the shifting of predominated diffraction peak should be explained and consequently, the peak shifting analysis is also carried for Mg doped samples for both as grown and annealed.

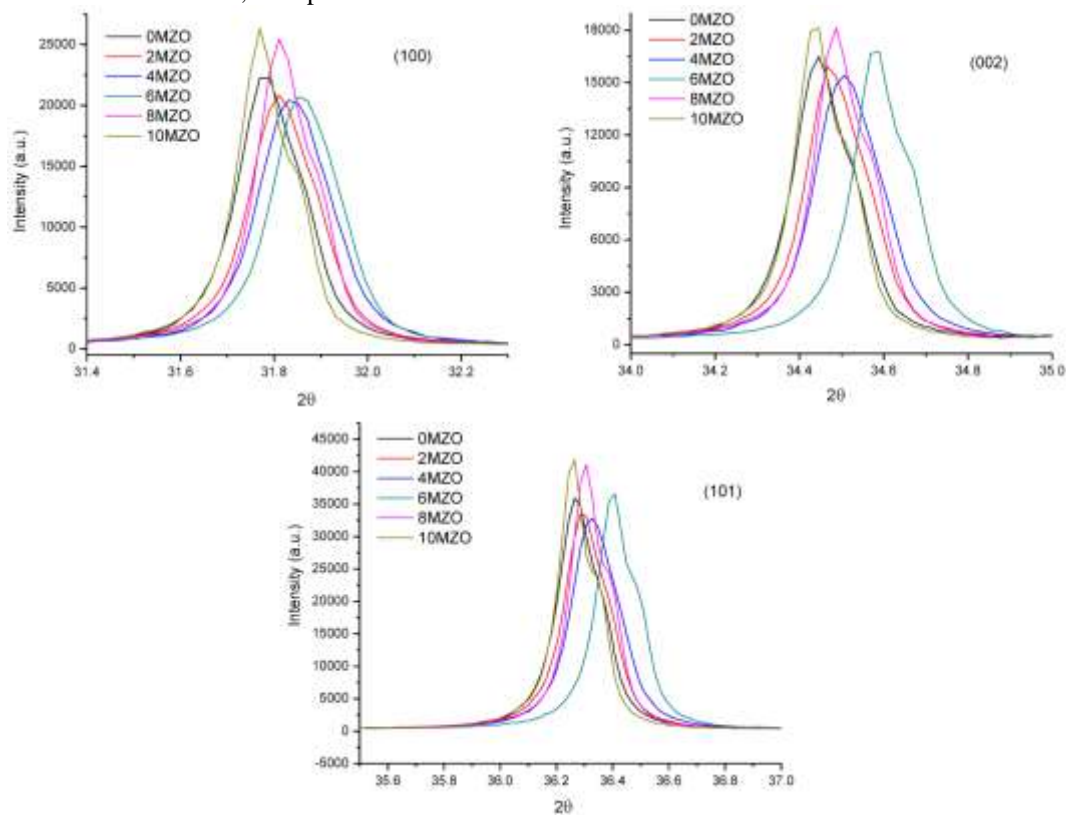


Fig 6. XRD spectra of (100), (002) & (101) oriented peaks of ZnO phases observed from 700°C annealed undoped and Mg doped ZnO nano particles

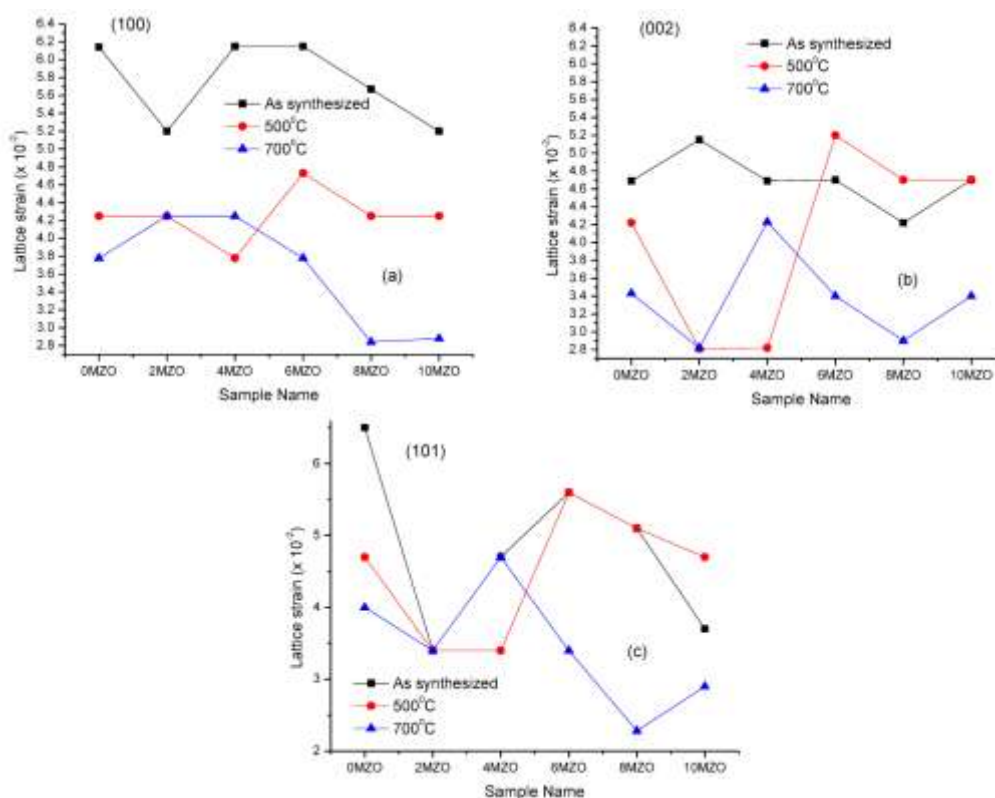


Fig 7. Variation in lattice strain of (a) (100), (b) (002) and (c) (101) oriented undoped and Mg doped ZnO nano particles at two different annealing temperatures.

Fig.5(a-c) shows the XRD spectra of (100), (002) & (101) oriented peaks of ZnO phases observed from 500°C annealed undoped and Mg doped ZnO nano particles and clearly depicts that the sample with 6% M Mg concentration shows noticeable peak shifting towards lower 2θ from the standard value. There is not distinguished peak shifting as the Mg concentration increases other than 6MZO. Meanwhile, noticeable peak shifting towards higher 2θ value was observed for the samples annealed at 700°C as shown in fig.6. The standard peak position shifts towards higher 2θ for the samples with $\leq 6M$ % of Mg in the synthesized samples. This observation was notice for all predominated orientations {(100), (002) & (101)} especially for (002) & (101) orientation. Distinguished peak shifting was noticed with 6MZO samples for (002) & (101) orientations (see fig.6). as increasing the Mg concentration $> 6M$ %, the predominated

peaks are shifting towards lower 2θ value and reaching the 2θ value of undoped ZnO (0MZO).

B. Crystallite size analysis

From the XRD data, the mean crystalline sizes (D) of the undoped and Mg doped ZnO nanoparticles were calculated by using the Debye Scherrer formula [13];

$$D = 0.9\lambda/\beta\cos\theta \quad (1)$$

where $\lambda = 1.5406 \text{ \AA}$ is the wavelength of the X-ray radiation used, θ is the Bragg diffraction angle of the XRD peak and β is the measured broadening of the diffraction line peak at an angle of 2θ , at half its maximum intensity (FWHM) in radian. For calculation, we considered only the 3 dominant peaks {(100), (002) and (101)} and calculated the crystallite size as given in table - 2. In order to get the exact value, the instrumental broadening was considered and used in this crystallite calculation. The FWHM of Si (111) oriented peak was recorded as 0.072 ($^{\circ}2\theta$) and used in this calculation.

TABLE II
CRYSTALLITE SIZE OF UNDOPED AND MG DOPED ZNO NANO PARTICLES

Samples	Average Crystallite size (nm)		
	As grown	Annealed at 500	Annealed at 700
0MZO	51	75	100
2MZO	77	125	125
4MZO	60	131	75
6MZO	54	58	109
8MZO	62	68	234
10MZO	74	71	154

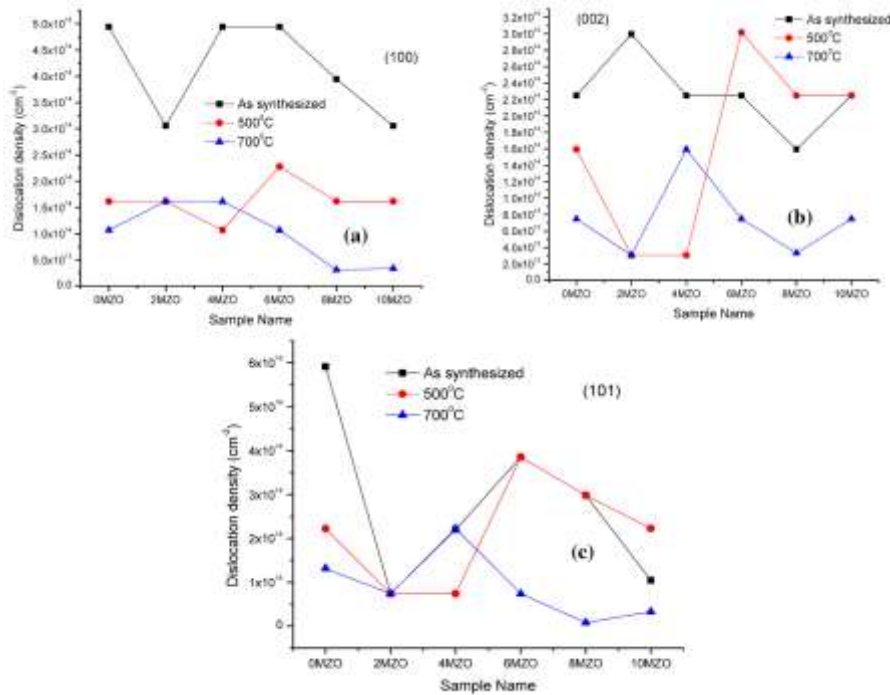


Fig 8. Variation in dislocation density of (a) (100), (b) (002) and (c) (101) oriented udoped and Mg doped ZnO nano particles at two different annealing temperatures.

From the table - 2, the as grown samples show the crystallite size value less than 100 nm. Moreover, on considering the Mg doping, the crystallite size increases with Mg concentration increases. As we know, the annealing temperatures supports to increase the crystallite size of the undoped and Mg doped ZnO samples. At 500°C, a small decrement in crystallite size is noticed with 10MZO samples. A gradual increase in crystallite size is observed for undoped samples at high annealing temperatures. Over all, the Mg doping influences the crystallite size and enhances the crystallite size of doped ZnO with increased Mg concentration. However, the peak broadening is as a result of defects and internal stress, so the mean crystalline size calculated by this method is normally smaller than the actual value [16]. In order to support this, the other structural parameters are analysed here.

C. Lattice strain analysis

The lattice strain (ϵ) has been determined by using the tangent formula [17]

$$\epsilon = \beta / (4 \tan\theta) \tag{2}$$

and the calculated values are plotted in fig.7. It clearly shows that the annealed samples show low lattice strain values than as grown samples. Fig 6 clearly explains the influence of Mg doping on lattice strain with respect to the crystal orientation of undoped and Mg doped samples. Fig 6 clearly indicates that the high annealing temperature suppress the lattice strain of ZnO in presence of Mg. On considering (100) orientation, at 700°C, the lattice strain values are decreasing with Mg concentration increasing. For (002) orientation at 500°C, the lattice

strain are shoot up for high Mg concentration (> 4M) in ZnO lattice and shows high value than as grown and annealed at 700°C samples. Moreover, low value in lattice strain is also notices with low Mg doped samples (2MZO & 4 MZO).

For (101) orientation, low value in lattice strain is observed for 8MZO sample at 700°C. On considering the change in lattice strain for different annealing temperatures at various Mg concentrations, similar pattern is noticed with annealed samples. Overall, the changes in lattice strain are not linear with respect to the Mg concentration.

D. Lattice Parameter Analysis

Change in lattice parameters is the evidence of expansion of the crystal lattice and are temperature dependent [18]. To understand the effect of Mg doping on lattice parameters of ZnO, the lattice parameters should be measured for undoped and doped ZnO nanoparticles. Since ZnO lattice is wurzite structure with hexagonal shape, there are two lattice parameters a and c are exist and can be measured by the following relations [19]:

$$d_{hkl} = \frac{1}{\sqrt{\frac{4(h^2+k^2+hk)}{3a^2} + \frac{l^2}{c^2}}} \tag{3}$$

$$a = \frac{\lambda}{\sqrt{3}\sin\theta} \tag{4}$$

$$c = \frac{\lambda}{\sin\theta} \tag{5}$$

where d is the interplaner distance, $\lambda = 1.5406 \text{ \AA}$ is the wavelength of the X-ray radiation used, θ is the

angle of the diffraction peak with respect to the orientation considered for calculation. Using the relation given in equation (4) and (5), the lattice parameters of undoped and Mg doped ZnO nano particles is calculated and the observed results are

summarized in table – 3. It is observed from the table – 3 that *a* and *c* values are increasing gradually with Mg concentration increasing upto 6M % (6MZO) for undoped ZnO nano particles.

TABLE III
CALCULATED LATTICE PARAMETERS AND CELL VOLUME FOR UNDOPED AND MG DOPED ZNO NANO PARTICLES AT DIFFERENT ANNEALING TEMPERATURES

Sample Name	As grown				500				700			
	a	c	c/a	Volume	a	c	c/a	Volume	a	c	c/a	Volume (Å ³)
0MZO	3.2418	5.1903	1.6010	47.238	3.2436	5.1961	1.6020	47.341	3.2485	5.2019	1.6013	47.540
2MZO	3.2465	5.2034	1.6028	47.495	3.2426	5.1961	1.6025	47.312	3.2455	5.1976	1.6015	47.413
4MZO	3.2475	5.2034	1.6023	47.524	3.2445	5.1976	1.6019	47.384	3.2426	5.1947	1.6020	47.299
6MZO	3.2485	5.2064	1.6027	47.580	3.2505	5.2049	1.6012	47.625	3.2406	5.1830	1.5994	47.135
8MZO	3.2386	5.1903	1.6026	47.143	3.2436	5.1947	1.6015	47.328	3.2455	5.1961	1.6010	47.399
10MZO	3.2445	5.1976	1.6019	47.383	3.2455	5.1990	1.6019	47.426	3.2495	5.2034	1.6013	47.583

After annealing, the lattice parameters values are increased for undoped ZnO nano particles. The increasing trend in lattice parameters was not observed for Mg doped samples. Moreover, decreasing in *a* and *c* values are noticed with Mg doped (upto 6M %) samples annealed at 700°C i.e, lattice parameters decreases with Mg concentration increases. These results are agreed with the published work [15]. A small increase in lattice parameters is also noticed with all samples having higher Mg concentration (≥8 M%) irrespective to the annealing temperatures. The lattice expansion is expected as a result of annealing and hence the increased lattice parameters are observed in our undoped and Mg doped samples. Very small change in *c/a* ratio is noticed for all samples and the calculated values are very close to the standard value (JCPDS 36-1451). Since there is a change in lattice parameters, the cell volume is anticipated and calculated by using the following relation:

$$V = 0.866 a^2c \quad (6)$$

The calculated values are given in the same table – 3. The expansion and contraction in ZnO lattice are noticed in all samples with respect to the lattice parameters. The calculated values are also depicted the influence of Mg on changing the volume of the cell of ZnO. The observed values are well agreed with the values reported in the literature [20].

E. Dislocation Density Analysis

A dislocation density is a measure of crystallographic defect or irregularity, within a crystal structure. It is also defined as a topological defect. The movement of a dislocation is impeded by other dislocations present in the sample. Thus, a larger dislocation density implies a larger hardness. The dislocation density δ stands for the magnitude of defects and can be determined by the following relation [21]:

$$\delta = 1/D^2 \quad (7)$$

where *D* is particle size (in nm). In our analysis, the dislocation density was calculated for three preferred

orientations of ZnO crystal {(100), (002) and (101)} of all samples and the observed data are plotted in fig.8.

From the equation (4), the dislocation density is purely dependent on the crystallite size of the synthesized nano particles. As we discussed for the crystallite size change, the same trend is observed for the dislocation too. The observed values are in between $10^{12}/m^2$ and $10^{14}/m^2$. From the fig 8, it clearly shows that the dislocation density varies with respect to the orientation of the crystal. Low value in δ was noticed for (101) orientated phase with 8MZO samples annealed at 700°C ($8.23 \times 10^{12}/m^2$). High value in δ was also noticed for (101) orientated phase with as grown 0MZO samples ($5.91 \times 10^{14}/m^2$). These values are less compared with the published values in literature [22]. So it is concluded that the Mg doping supports to decrease the dislocation density of ZnO nano particles at annealed conditions. Moreover, the as grown samples are also show low value compared to the published value [23].

F. Residual Stress Analysis

Residual stress is possible at the time of crystal growth and also during the annealing process. This kind of stress is developing during manufacturing and processing of materials where the heterogeneous plastic deformations, thermal contractions and phase transformations occur in the nano size materials.

TABLE IV
VARIATION IN STRESS DEVELOPED IN UNDOPED AND MG DOPED ZnO NANO PARTICLES AT DIFFERENT ANNEALING TEMPERATURES

Sample Name	As grown			500			700		
	(100)	(002)	(101)	(100)	(002)	(101)	(100)	(002)	(101)
0MZO	0.036935	0.037778	0.023803	0.01401	0.013941	0.002896	-0.01839	0.00611	-0.00416
2MZO	-0.00517	0.004905	-0.00344	0.020139	0.018416	0.027242	0.000876	0.006024	0.009503
4MZO	-0.01226	-0.01489	-0.01457	0.006209	0.006024	0.0162	0.021095	0.021858	0.009322
6MZO	0.019025	0.025988	0.045253	0.032955	0.02246	0.03222	0.033353	0.09182	0.074576
8MZO	0.044975	0.041392	0.033849	0.013453	0.01962	0.01077	0.003502	0.03227	0.016743
10MZO	0.008358	0.009294	-0.00833	0.00207	0.005594	-0.00643	-0.00716	0.001291	-0.00968

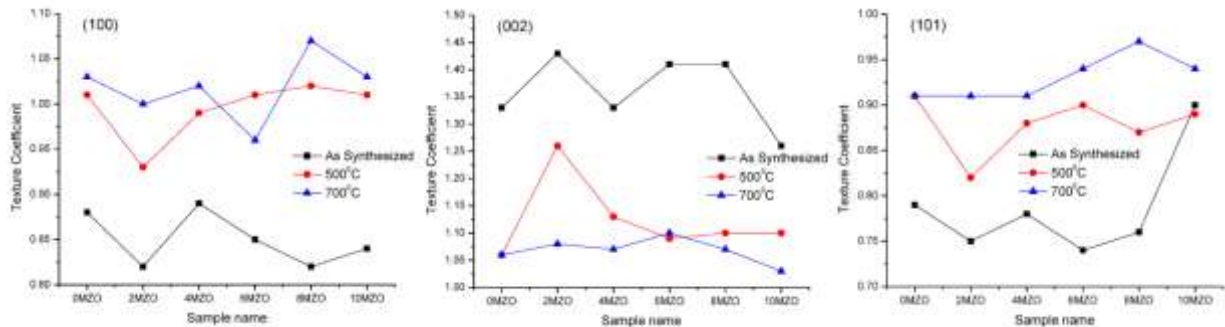


Figure 9. Variation in texture coefficient of (100), (002) and (101) oriented udoped and Mg doped ZnO nano particles at two different annealing temperatures.

The plastic deformation and thermal contractions are expected since undoped and Mg doped ZnO nano particles undergone for annealing process. Moreover, the doping process may influence the residual stress of bare materials. So it has to be addressed for clear understanding the influence of doping and annealing on the change in residual stress of ZnO in this study. Consequently, the residual stress is evaluated using the following equation [23];

$$\sigma = -E (d_a - d_o) / (2d_o Y) \quad (8)$$

where E and Y are the Young's modulus (128GPa) and the Poisson's ratio (0.35) of ZnO respectively [24]. d_a and d_o are the d spacing of bulk and ZnO nano particles from JCPDS data. Residual stress is classified into two: a) tensile stress is the stress that can be applied to an object by pulling on it, or attempting to stretch it. Positive values of stress indicate tensile stress. b) Compressive stress is the stress applied to materials resulting to their compaction (decrease of volume). Negative values of stress indicate compressive stress. The stress developed during the process was measured by using the relation (8) and the observed values are given in table – 4. In this analysis, the preferred and predominant peaks are considered as we mention in the previous discussion.

From the table – 4, the stress values are changing with respect to orientation, doping and annealing temperatures. On considering the results of 500°C, all stress generated in the undoped and Mg doped nano particles are tensile in nature except (101) oriented phase. On considering the Mg concentrations, 10MZO

samples show reduced tensile stress at 500 °C and also observed the conversion from tensile to compressive when it undergoes at high temperature annealing (700°C) for (100) orientation. For (002) orientation of 10MZO, stress is decreases with temperature increases. The same behaviour is also noticed with 0MZO samples. On increasing Mg concentration, conversion from tensile to compressive is observed for 2MZO and 4MZO samples at asgrown condition for both (100) and (101) orientations. The changes in stress values are random for their respective orientations. Over all, high and low values in tensile stress are noticed with (002) orientation of 6MZO samples (9.18×10^{-2}) and (100) orientation of 2MZO samples (8.76×10^{-4}) respectively when annealed at 700°C.

G. Texture Coefficient Analysis

On synthesis of nano materials, grow of crystals and their preferred growth are more important for the specific application. Consequently, from the XRD spectra analysis, the preferred growth could be validated by studying the texture coefficient analysis by using the equation (9) as follows [25]:

$$P_i (TC) = N (I_i / I_o) / \sum (I_i / I_o) \quad (9)$$

Where P_i is the Texture Coefficient of the plane I , I_i is the measured intensity, I_o is the intensity of the JCPDS powder diffraction pattern of the corresponding peak and N is the number of reflections considered for the analysis. When P_i is greater than unity, it is indicating that the peak is preferred orientation of the crystallites in that particular

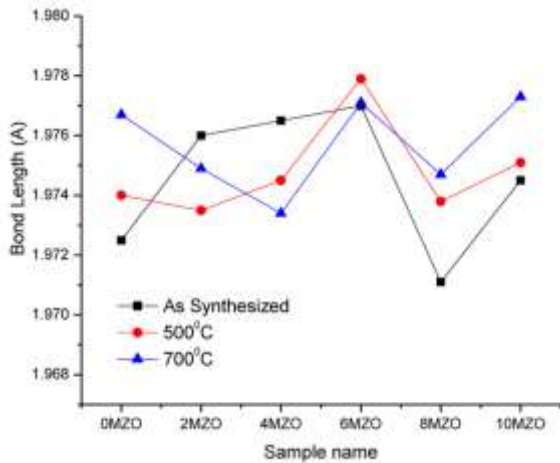


Fig.10 Change in bond length of Zn-O with influence of Mg in ZnO lattice for various Mg concentrations and processing temperatures

direction. In this analysis, three reflections are considered and the observed data are plotted against the Mg doping concentration and the annealing temperature as shown in fig 9.

Fig.9 depicts that the (002) orientation is the preferred growth in their direction for all Mg concentrations and annealing temperatures. But the annealing process is not supporting to grow with (002) orientations for all doping concentrations. It is confirmed by observing low value in TC for annealed samples. On considering (100) orientation, Mg doping supports the growth with their preferred orientation when annealed the samples at 700°C. It is also noticed that for (101) orientation, the TC values are less than 1 for all samples irrespective to the Mg concentration and also the annealing temperature and considered as randomly oriented crystals in their direction. Overall the preferred growth is observed for (002) orientations for all samples at as-grown condition and showed the TC values > 1.25.

H. Bond Length Analysis

In the crystal lattice, the bond length is a key parameter and will change with respect to the process conditions and also the doping element. In doping process, the bond length of ZnO crystal will change and should be addressed for various doping concentrations. In this study, Mg was doped into ZnO and influenced the bond length of ZnO. For hexagonal structure of ZnO, the Zn-O bond length *L* is calculated using the following relations as suggested in the literatures [26,27].

$$L = \sqrt{\left[\frac{a^2}{3} + \left(\frac{1}{2} - u \right)^2 c^2 \right]} \tag{10}$$

Where

$$u = \frac{a^2}{3c^2} + 0.25 \tag{11}$$

Form the relations (10) and (11), it is clearly seen that the bond length is mainly depending on the lattice parameters of the synthesized nano particles. From the lattice parameter values of undoped and Mg doped

ZnO nano particles, the bond length is calculated and plotted in fig.10. It clearly shows that the bond length gradually increases with Mg concentration increases. Sudden drop in bond length was noticed with 8M % of Mg (8MZO) for as grown sample. For samples 0MZO, 8MZO and 10MZO, annealing temperatures aid to increase the bond length of Zn-O bond. For as grown and annealed conditions, up and down values of bond length is noticed for 2MZO, 4MZO and 6MZO. For 6MZO sample at as grown and annealed condition (500°C), the observed bond length value (1.9778 Å) is well agreed with the bulk value of ZnO bond length (1.9778Å) [26]. In addition to this, the annealed 10MZO samples at 500 and 700°C also show the bond length value close to the bulk one.

IV. CONCLUSION

Undoped and Mg doped ZnO nanoparticles were synthesized by precipitation method and their structural parameters were analysed using the XRD data. The peak intensity of preferred orientations of ZnO phase was affected by Mg doping and also annealing. The crystallite size was varied in between 51 and 77 nm for as synthesized samples. Preferred oriented peak shifting was noticed with annealed samples especially for 6M % of Mg concentrated samples. High value lattice parameter was noticed with ≥8M % of Mg in ZnO. From the texture coefficient analysis, (002) oriented ZnO was evidenced as preferred growth which was suppressed by annealing process. ZnO nano particles with low dislocation density (8.23 x 10¹²/m²) were successfully synthesized using 8% M (8MZO) with help of annealing process at 700°C. Non-linear change in bond length was observed and low value in bond length was noticed for all Mg doped samples irrespective to the synthesis conditions.

REFERENCES

- [1] Nano.gov (2015), *What It Is and How It Works*, Nano. <http://www.nano.gov/nanotech-101/what> Accessed 14 March 2015.
- [2] A.K. Radzimska and T. Jesionowski, "Zinc Oxide— From Synthesis to Application: A Review," *Materials* vol. 7, pp. 2833 - 2881, April 2014.
- [3] I.J. No, D.Y. Jeong, S. Lee, S.H. Kim, J.W. Cho, P.K. Shin, "Enhanced charge generation of the ZnO nanowires/PZT hetero-junction based nanogenerator," *Microelect. Engg* vol. 110, pp. 282-287, Oct. 2013.
- [4] S. Pearton, C. Abernathy, D. Norton, A. Hebard, Y. Park, L. Boatner and J. Budai, "Advances in wide bandgap materials for semiconductor spintronics," *Mater. Sci. Engg R: Reports* vol. 40, pp. 137-168, Feb. 2003.
- [5] L.L. Yang, Q.X. Zhao, and M. Willander, "Size-controlled growth of well-aligned ZnO nanorod arrays with two-step chemical bath deposition method," *J. Alloys and Comp.* vol. 469, pp. 623 - 629, Feb. 2009.
- [6] B. Gopal Krishna, M. Jagannadha Rao, "Biosynthesis and measurement of thermal conductivity of ZnO material", *International Journal of Engineering Trends and Technology*, vol. 26(5), pp. 272-275, Aug. 2015.
- [7] C. Jagadish and S. Pearton, *Zinc oxide bulk, thin films and nanostructures*, Amsterdam, Elsevier, 2006.
- [8] K. Omri, I. Najeh, R. Dhahri, J. El Ghoual and L. El Mir, Effects of temperature on the optical and

- electrical properties of ZnO nanoparticles synthesized by sol-gel method,” *Microelect. Engg.*, vol. 128, pp. 53- 58. Oct. 2014.
- [9] D. Raoufi, “Synthesis and microstructural properties of ZnO nanoparticles prepared by precipitation method,” *Renewable Energy* vol. 50, pp. 932-937, Feb. 2013.
- [10] S. Kumar, P.D. Sahare, “Observation of band gap and surface defects of ZnO nanoparticles synthesized via hydrothermal route at different reaction temperature,” *Optics Commu.* vol. 285, pp. 5210 - 5216. Nov. 2012.
- [11] Y. Chen, C. Zhang, W. Huang, Y. Situ, H. Huang, “Multimorphologies nano-ZnO preparing through a simple solvothermal method for photocatalytic application,” *Mater. Lett.* vol. 141, pp. 294-297, Feb. 2015.
- [12] H.R. Ghaffarian, M. Saiedi, M.A. Sayyadnejad, and A.M. Rashidi “Synthesis of ZnO Nanoparticles by Spray Pyrolysis Method,” *Iran, J. Chem. Chem. Engg.* vol. 30, pp.1-6, Oct. 2011.
- [13] S.S Alias, A.B. Ismail and A.A. Mohamad, “Effect of pH on ZnO nanoparticle properties synthesized by sol-gel centrifugation,” *J. of Alloys and Comp.* vol. 499, pp. 231 – 237, June 2010.
- [14] V. Etacheri, R. Roshan and V. Kumar, “Mg-doped ZnO nanoparticles for efficient sunlight-driven photocatalysis,” *ACS Appl. Mater. & Inter.* vol. 4, pp. 2717 - 2725, May 2012.
- [15] M. Arshad, M.M. Ansari, A. Ahmed, P. Tripathi, S. Ashraf, A. Naqvi and A. Azam, “Band gap engineering and enhanced photoluminescence of Mg doped ZnO nanoparticles synthesized by wet chemical route,” *J. Luminescence*, vol. 161, pp. 275 - 280, May 2015.
- [16] A. Ashour, M.A. Kaid, N.Z. El-Sayed, A.A.Ibrahim, “Physical properties of ZnO thin films deposited by spray pyrolysis technique,” *Appl. Surf. Sci.* vol. 252, pp. 7844-7848, Sept. 2006.
- [17] H.P. Klug and L.E. Alexander, *X-Ray Diffraction Procedures for Polycrystalline and Amorphous Materials*, Wiley, New York. 1974.
- [18] P. Singh, A. Kumar, Deepak, D. Kaur, “ZnO nanocrystalline powder synthesized by ultrasonic mist-chemical vapour deposition,” *Opt. Mater.* vol. 30, pp. 1316 – 1322, April 2008.
- [19] M.A. Gondal, Q.A. Drmosh, Z.H. Yamani, T.A. Saleh, “Synthesis of ZnO₂ nanoparticles by laser ablation in liquid and their annealing transformation into ZnO nanoparticles,” *Appl. Surf. Sci.* vol. 256, pp. 298 - 304, Oct. 2009.
- [20] A.K. Zak, Abd. W.H. Majid, M.E. Abrishami and Ramin Yousefi “X-ray analysis of ZnO nanoparticles by Williamson-Hall and size-strain plot methods,” *Sol. State Sci.*, vol. 13, pp. 251 - 256 . Jan. 2011.
- [21] X.S. Wang, Z.C. Wu, J.F. Webb, Z.G. Liu, “Ferroelectric and dielectric properties of Li-doped ZnO thin films prepared by pulsed laser deposition,” *Appl. Phys. A*, vol. 77, pp. 561 - 565 . Aug. 2003.
- [22] A.J. Perry, “The state of residual-stress in Tin films made by physical vapor-deposition methods - the state-of-the-art,” *J. Vac. Sci. Technol.* vol. 8, pp. 1351 - 1358 , Sep. 1990.
- [23] M. Mazhdi and P. Hossein Khani, “Structural characterization of ZnO and ZnO:Mn nanoparticles prepared by reverse micelle method,” *Int. J. Nano Dimens.* vol 2. pp. 233 - 240, Nov. 2012.
- [24] S. Adachi, “*Handbook on Physical Properties of Semiconductors*,” Kluwer Academic Publisher, Boston, pp 72. 2004.
- [25] H. Hadouda, J. Pouzet, J.C. Bernede and A. Barreau, “MoS₂ Thin Film Synthesis by Soft Sulfurization of a Molybdenum Layer,” *Mat. Chem. Phys.*, vol.42, pp. 291 - 297, Dec. 1995.
- [26] S. Ilıcan, Y. Caglar and M. Caglar, “Preparation and characterization of ZnO thin films deposited by sol-gel spin coating method,” *J. Optoelectron. Adv. Mater.* vol. 10, pp. 2578 - 2583 , Oct.2008.
- [27] Barret CS, Massalski TB, “*Structure of Metals*,” Pergamon Press, Oxford. 1980.